AIP | Physics of Fluids

A novel simplified Bernoulli trials collision scheme in the direct simulation Monte Carlo with intelligence over particle distances

Bijan Goshayeshi, Ehsan Roohi, and Stefan Stefanov

Citation: Physics of Fluids **27**, 107104 (2015); doi: 10.1063/1.4933251
View online: http://dx.doi.org/10.1063/1.4933251
View Table of Contents: http://scitation.aip.org/content/aip/journal/pof2/27/10?ver=pdfcov
Published by the AIP Publishing

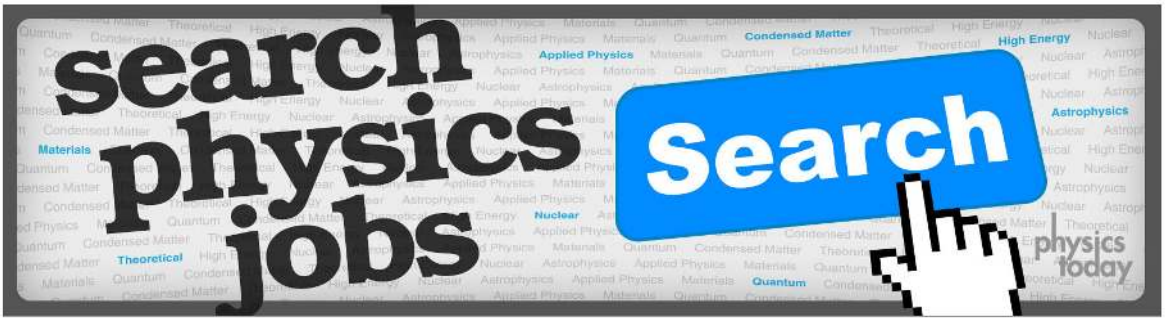

PHYSICS OF FLUIDS **27**, 107104 (2015)

A novel simplified Bernoulli trials collision scheme in the direct simulation Monte Carlo with intelligence over particle distances

Bijan Goshayeshi,[1] Ehsan Roohi,[1,a)] and Stefan Stefanov[2]
[1]*High Performance Computing (HPC) Laboratory, Department of Mechanical Engineering, Ferdowsi University of Mashhad, P.O. Box: 91775-1111, Mashhad, Iran*
[2]*Institute of Mechanics, Bulgarian Academy of Science, Acad. G. Bontchev Str., 1113 Sofia, Bulgaria*

(Received 23 April 2015; accepted 5 October 2015; published online 21 October 2015)

This work deals with the development of an intelligent inter-particle collision scheme using the Direct Simulation Monte Carlo (DSMC) method. Conventional DSMC collision schemes cannot perceive collision distances by their own routines and, consequently, must rely on other techniques to provide a choice of collision pairs with a smaller inter-particle space. Here, we propose a modification of the Simplified Bernoulli Trials (SBT) scheme, called the Intelligent Simplified Bernoulli Trials (ISBT) scheme, which can create pseudo-circular subcells that reduce approximately 25%–32% of the mean collision separation distance. The ISBT scheme tries to arrange the particle indexing and collision acceptance-rejection of the SBT scheme in a way that leads to the formation of virtual clusters. These inner-cell clusters then will cause the selection of the "near-neighbor" pair, which leads to smaller mean collision separation distances. Different low- and high-speed test cases, e.g., lid-driven cavity flow, steady hypersonic flow over a two-dimensional cylinder, and Mach 15.6 nitrogen flow over a 25°–55° axisymmetric biconic, are selected to assess the accuracy and efficiency of the ISBT collision scheme. [http://dx.doi.org/10.1063/1.4933251]

I. INTRODUCTION

The Direct Simulation Monte Carlo (DSMC) is a particle-based method, developed by Bird,[1,2] that simulates the rarefied gas flows. In this scheme, the solution of the Boltzmann equation is obtained through deterministic-statistical approaches. The primary principle of the DSMC method is to decouple the motion and collision during a time step Δt into two sequential stages of free-molecular movement and then collision. Implementation of the DSMC method requires breaking down the computational domain into a collection of grid cells. The size of each cell should be sufficiently small to result in small variation in thermodynamic properties within each cell. The cells are divided into sub-cells in each direction. Sub-cells are then utilized to facilitate the selection of collision pairs. After fulfilling all molecular movements, the collisions between molecules are simulated in each cell independently. Wagner[3] proved that if the number of simulators tends toward infinity while the time step and the grid size become close to zero, the DSMC method faithfully solves the Boltzmann equation. It is evident that the stochastic binary collision scheme plays a major role in the DSMC method. Theoretical investigation into the construction of a collision scheme can be categorized into two groups. Design of the first group is based on the principle of the maximum collision rate per time step, e.g., "No Time Counter (NTC),"[2] "null-collision,"[4] and "majorant frequency scheme."[5] In this group, the Bird's NTC scheme has been widely used as a

a)Author to whom correspondence should be addressed. Electronic mail: e.roohi@ferdowsi.um.ac.ir. Tel.: +98 (51) 38805136. Fax: +98 (051) 38763304.

highly reliable scheme. Since the collision pairs in this scheme are merely chosen through random selections, NTC requires a number of particles in the cell that is suitable/high enough to avoid successively repeated collisions. The second type of collision schemes known as the "Bernoulli trials," proposed by Belotserkovskii and Yanitiskiy[6] and Yanitiskiy,[7] are constructed on the basis of the Kac stochastic model. Contrary to the first group of collision schemes, the latter group in accordance with the Kac stochastic model defines a collision probability function for each particle pair and checks all pair combinations for collision occurrence; hence, it avoids at least part of the successively repeated collisions. However, the quadratic dependency of the computational cost on the particle number in cells makes this algorithm considerably less efficient than the traditional collision schemes. Recently, Stefanov[8,9] proposed a modified version of the Bernoulli trial scheme called "simplified Bernoulli-trials," or SBT, which removes the quadratic dependency and makes the computational performance of the collision algorithm linear with respect to the number of particles in cells. SBT scheme faithfully solved a wide spectrum of rarefied flow problems using a quite small number of simulator particles.[10–12] It has been well-known that the quality of the collisions and consequently the accuracy of the results are mainly dependent on the collision separation distances. The reduction effect of large collision separation distance on the average angular momentum has been the chief motive of the following developments in the DSMC community. LeBeau *et al.*[13] introduced the "virtual subcell" (VSC) method, in which the nearest neighbor (NN) partner of a given particle will be found and selected. VSC needs the collision separation examination of all the available particles in the cell to find the nearest neighbor one. The implementation of this method in the second group of collision schemes is not possible, because the partner selection in these schemes is bounded to definite referenced particles, e.g., a list consisting of a portion of available particles. Bird[14] proposed static subcells, in which collision pairs had to be chosen from their own or neighboring subcells. Stefanov *et al.*[15,16] suggested the idea of dynamic subdivision of collision cells. They adjusted the subcell in a way that the subcell size remains smaller than the mean free path (λ) at every time step. In order to provide a sufficient number of subcells that is compatible with the instantaneous number of particles inside each collision cell, Bird proposed the transient adaptive subcell (TAS) technique.[17,18] Since then, TAS technique has been successfully employed both by the first group,[19–21] and also by the second group[22–24] of collision schemes. However, due to the inherent limits in the procedure of the second group of collision schemes, the TAS implementation cannot search for a partner through neighbor subcells; therefore, the adaptation was based on more than one "Particle Per Subcell (PPSC)," e.g., PPSC = 4–5.[24] The aforementioned developments in the reduction of the collision separation distance are all gained by implementing some extra techniques, i.e., the collision scheme itself is unable to perceive the near partner. Thus, having a collision scheme that tries to recognize a closer partner is the major goal of this paper. On the other hand, Gallis *et al.*[25–27] showed that the selection of the nearest neighbor partner may give rise to new sources of error. Their assessment on the nearest neighbor partner-selection implies that the mentioned policy in the partner selection requires stringent temporal discretization. In fact, an insufficiently small value of the time step would cause particles to ignore some of their probable collision-pairs in their advection phase of the simulation. As a result, in order to increase the efficiency and accuracy of a collision scheme, they suggested using the policy of near neighbor rather than of nearest neighbor. Understanding this fact, our modifications also aim at a collision scheme that considers near neighbor selection. To meet this desire, the SBT from the second group of collision schemes is chosen as a basis to create the Intelligent Simplified Bernoulli Trials (ISBT) scheme. The DS2V code version 4.5.09, released with the Bird newest monograph[28] is selected as the basic code for modifications. The collision routine in this code[29,30] benefits from the VSC and TAS techniques when searching for the nearest neighbor partner, while it inherits the fundamentals of the NTC method, e.g., how to estimate the number of collisions. Therefore, it seems to be abbreviated as "NTC-NN," but following Bird,[28] we call it here just as the "NN" method. In this work, the NN collision scheme and the TAS subroutine of the DS2V code are substituted by the corresponding SBT-TAS and ISBT-TAS subroutines. To validate the ISBT scheme, we investigated its features, e.g., collision frequency at the equilibrium state and mean collision separation (MCS) in the lid-driven cavity flow. Our first test case, the Mach 10 lid-driven cavity flow deals with the investigation of the angular momentum conservation in high-velocity forced-vortical flows.

Furthermore, we investigated the ISBT-TAS behavior over hypersonic test cases, including steady hypersonic flow over a two-dimensional cylinder and axisymmetric flow over the biconic. Mach 10 lid-driven cavity flow is a suitable test in which the collision scheme is exposed to rapid changes of the angular momentum. Hypersonic flow passing over a cylinder is a well-known benchmark, first considered by Lofthouse *et al.*,[31] and then considered as a challenging test case for different DSMC solvers.[19–21,23,24,28,32] In addition, Mach 15.6 nitrogen flow over a 25°–55° axisymmetric biconic geometry, whose experimental[33,34] and numerical data[26,35] were reported in the literature, is considered. This test case contains high-speed low-density regions, laminar recirculation zone, and interactions between shock waves and separated-flow. We compared the ISBT-TAS and its preliminary SBT-TAS solutions with that of the original, nearest neighbor algorithm of DS2V, called benchmark solution, as well as with the experimental data, where available.

II. NUMERICAL METHOD

The DSMC program used in this study is the DS2V program of Bird.[28] It benefits from the classical Larsen-Borgnakke model for rotational degrees of freedom, while the quantum Larsen-Borgnakke model is employed for the vibrational modes. The molecular model for simulation of collisions in this study is the variable hard-sphere (VHS) model.

A. Collision scheme

1. NN scheme

DS2V code benefits from one of the state-of-the-art collision schemes called NN, which fundamentally obeys the NTC[2,36] scheme in assigning the maximum available number of pair selections (N_{pair}) within the cell space,

$$N_{pair} = \frac{1}{2} F_n N_c \left(N_c - 1\right) (\sigma g)^c_{max} \frac{\Delta t}{\forall_c}, \tag{1}$$

where $F_n, N_c, \forall_c$, and $(\sigma g)^c_{max}$, respectively, are the ratio of the number of real molecules to the simulated particles, the number of available particles within the collision cell, volume of the collision cell, and maximum value of the product of collision cross section and particles' relative velocities. The relation of the collision process to the Poisson distribution and its consequence, equality $\langle N_c \left(N_c - 1\right)\rangle = \langle N_c\rangle^2$, were pointed out by Yanitskiy,[7] then reemphasized and utilized in Eq. (1) by Stefanov and Cercignani,[37] and also presented by Bird in his sophisticated algorithm;[28] note that the Equation (1) is the modified expression of the Bird's original N_{pair} statement[36] and is derived by replacement of $[N_c \langle N_c\rangle]$ with $[N_c \left(N_c - 1\right)]$, where the operator $\langle\ \rangle$ denotes average over time. In the NN method, the first particle is chosen at random, and the second particle is chosen from the available nearest neighbors.[17] For doing so, DS2V provides two different techniques, TAS and virtual subcell. The latter performs $O(N_c{}^2)$ operations to sort all N_c particles in a cell to find the nearest-neighbor of any particle selected for collision. In the former scheme, cells are divided into transient sub-cells and collision partners are selected from the same or neighboring sub-cells instead of from everywhere in the cell. The decision of which of these two techniques to use depends on the available number of particles within that cell. LeBeau[13] demonstrated that for a small number of particles, say $N_c \leq 10$, virtual subcells can be an efficient approach. Furthermore, DS2V is designed in a way that it uses the virtual cell technique for $N_c < 40$. Transient adaptive subcell is an efficient alternative technique when there is a highly populated collision cell. In this situation, DS2V uses TAS instead of virtual cell to boost its computational efficiency. Once selected, the particle pair is checked for collision by using the acceptance-rejection procedure. The acceptance-rejection logic is set up on a probabilistic concept. For a chosen pair $1 \leq (i, j) \leq N_c$, the collision occurs if

$$\frac{(\sigma g)_{ij}}{(\sigma g)_{max}} \geq Ranf, \tag{2}$$

where σ is the collision cross section, g is the relative velocity of colliding particles, and *Ranf* is a random number between 0 and 1.

2. SBT scheme and its evolution to an intelligence over particle distances

a. The SBT scheme. The SBT scheme realizes the binary collisions without calculating the maximum number of eventual collisions beforehand. In this scheme, each particle has a chance to find its collision-pair among all available particles within the cell and the collision occurrence is ruled by a probability function, i.e., all of these happenings are conducted in a probabilistic context. However, these selections do not take into account the inter-particle distances and are just based on random selections. In order to bias selections toward closer partners, SBT scheme should be reconsidered via its indexing and acceptance-rejection sections. The SBT procedure starts with a locally indexing of N_c particles in the c-th cell from 1 to N_c. The first particle, say i, is sequentially selected from 1 to N_c, while its pair, say j, at each sequent is randomly selected among the further available particles, by considering this rule

$$j = (i+1) + int\left(Ranf_I \times (N_c - i)\right). \tag{3}$$

Eventually, the collision is accepted if its probability function, W_{ij},

$$W_{ij} = F_n\,(N_c - i)\,(\sigma g)_{ij}\frac{\Delta t}{\forall_c}, \tag{4}$$

fulfills the condition given by the following inequality:

$$W_{ij} \geq Ranf_{II}, \tag{5}$$

where $Ranf_I$ and $Ranf_{II}$ are random numbers between 0 and 1.

It is worth noting that the probability for $W_{ij} > 1$ should be kept always close to zero by choosing appropriate time step and cell size. The SBT scheme prevents at least part of repeated collisions, for more details, see Refs. 8 and 9.

b. ISBT. Here, we propose a variant of the SBT collision scheme, which increases the collision acceptance in favor of closer-pairs. ISBT is based on the simple idea of easier collision-acceptance for the closer pairs and more difficult collision-acceptance for the more separated ones. Therefore, it needs a system to calculate or estimate the inter-particle distances, and a system that regulates the acceptance-rejection in favor of closer pairs. The following procedure describes the evolution of SBT into ISBT scheme:

(i) The aim of the first step is to define a method for a locally indexing of particles based on the estimated inter-particle distances. The particle indexing should be modified in a way that a semi-perception of distance emerges in a hierarchical order of indexed numbers, i.e., in a collision cell with N_c particles, we need to have an indexing method that satisfies the condition of $\left(\delta_i < \delta_j, 0 < i < j \leq N_c\right)$, where δ_i is the distance of the ith particle to a reference point® (see Fig. 1(a)). One can easily observe that the indexed points, relative to their hierarchical order, would be closer to each other if points are located in the list with respect to the distance to the corners of a rectangle that surrounds the particles (compare Figs. 1(b) and 1(c), for example). Therefore, we suggest the random selection of cell/subcell corners to efficiently index particles. However, because the δ distance does not consider the angular distances, some particles continue to be indexed successively while they are far from one another. Specifically, this is seen for those particles on opposite sides of the diagonal (e.g., particles 4 and 5 in the Fig. 1(c)). Statistically, these particles are not the majority, yet any other means of particle indexing would inevitably create situations where indexed particles would be far from each other. Along the indexing direction (i.e., the diagonal RB in Fig. 1(a)), particles are prevented from colliding in opposite corners (because they are indexed at the bottom and the top of the hierarchical order), yet along the other diagonal (AC), particles might be indexed as neighbors, and their collision might reverse the angular momentum. Since these kinds of collisions might be inevitably supported in the ISBT scheme, we suggest using elongated cell/subcells as a solution. In a quadrangular cell/subcell ("RABC" in Fig. 1(d)), the

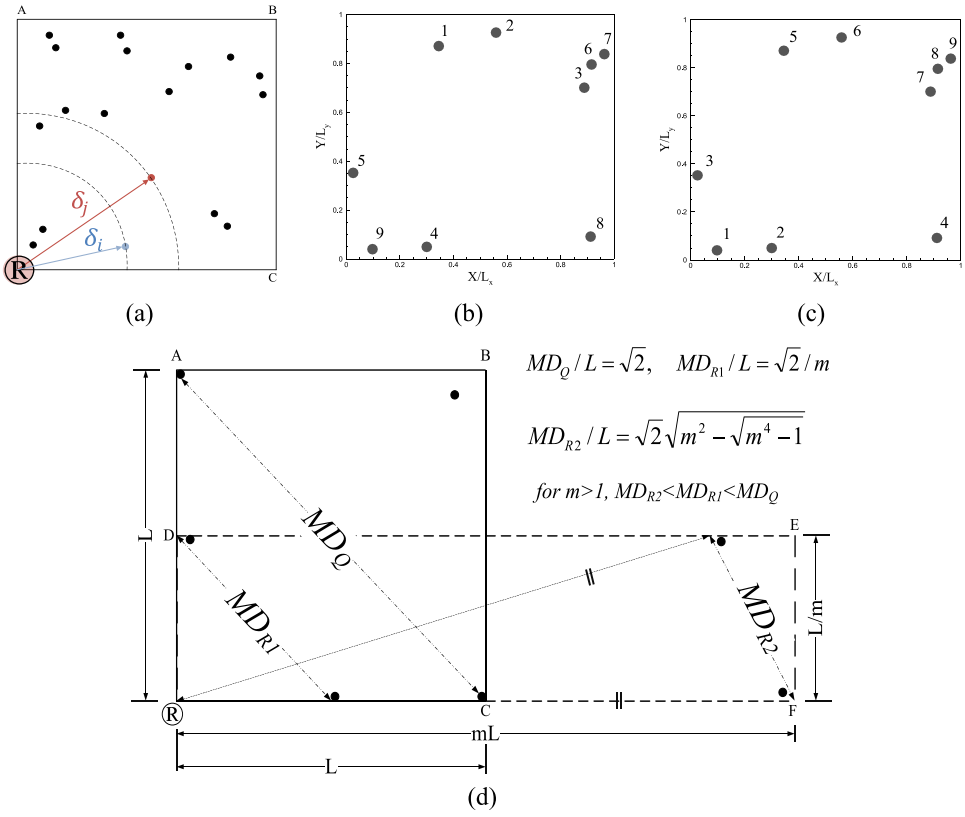

FIG. 1. Distribution of some particles in a cell/subcell; (a) a system of particle indexing based on the distance of particles to a definite center point®, (b) the indexing results for a group of nine particles when the ® is located on the center of the cell, (c) when this point is on the left-down corner of the cell, and (d) the geometrical comparison between one quadrangle cell/subcell ("RABC") and its equal-area elongated cell/subcell ("RDEF"), while the calculated values for the *MD* between two far-indexed particles are shown; they denote that elongated cell/subcell has smaller *MD* value.

maximum distance (*MD*) that two far-indexed particles could have is $\sqrt{2}$ times greater than the side length, i.e., diagonal of the quadrangle. It can be shown that, the corresponding values in the elongated rectangular cell/subcell ("RDEF" in Fig. 1(d)) will be smaller than those of an equal-area quadrangle (compare the MD_Q value of "RABC" quadrangle and maximum corresponding value MD_{R1} of "RDEF" elongated-rectangle). However, the use of elongated cell/subcell imposes the time step to be reduced accordingly. Therefore, in cases of hypersonic shock interaction simulations, we suggest using elongated cells/subcells with elongation factor two ($m = 2$), while the time step is better to be reduced about one third. Thus, the TAS technique is implemented in the present study as it was explained in detail in Ref. 24. For each cell, the transient layer of subcells is fabricated by a special number of divisions along x (D_x) and y (D_y), while the elongation direction changes randomly in each cell. As an example of x-direction elongation, these calculations are provided as follows:

$$D_x = \sqrt{\frac{m \times N_c}{AR \times Envelop \times PPSC}}, \tag{6}$$

$$D_y = D_x \times \left(\frac{AR}{m}\right), \; AR = \frac{\Delta y_{cell}}{\Delta x_{cell}}, Envelop = \frac{\forall_c}{\Delta y_{cell} \times \Delta x_{cell}}, \tag{7}$$

where *AR* is the aspect ratio of the cell, *m* is the elongation factor, *PPSC* is the assumed desired number of particles per subcell in the TAS adaptation, and *Envelop* is used to increase the number of subcells in case that the cell is not fully rectangular. It should be noted that

the bigger number for *PPSC* will create subcells with larger size, since there will be smaller number of subcells in a cell (see Equation (6)).

(ii) In the second step, the objective is to alter the acceptance-rejection method of the SBT scheme in favor of the selection of closer pairs. To perform this as simple as possible, the ISBT scheme just follows the SBT procedure, i.e., the first particle, say i, is sequentially selected from 1 to N_c, while its pair, say j, at each sequent is randomly selected among the further available particles, by considering the rule stated in Equation (3). The only difference is that instead of regenerating the second random number ($Ranf_{II}$), which was used in the acceptance-rejection section of the SBT scheme, here ISBT does not call any new random number and implements the first generated one ($Ranf_I$) for collision acceptance,

$$W_{ij} \geq Ranf_I, \tag{8}$$

where W_{ij} is calculated through Equation (4). Figure 2 compares the sequences of the ISBT and SBT procedures.

As a result of this modification, pseudo-circular subcells (Fig. 3) will be created that allow an easier acceptance for closer-pairs (because closer-pairs have been selected with $Ranf_I$ that has a smaller value, and therefore the right-hand side of inequality condition given by Eq. (8) would be smaller) and a more superior condition for far from each other particles (because these-pairs will be selected with $Ranf_I$ that has a larger value, and, respectively, the right hand side of Eq. (8) would be larger). In other words, a smaller number for j, as a second particle in the hierarchical list of indexed numbers, is only obtained if the $Ranf_I$ is closer to zero, and conversely, a greater number for j, as a second particle, is simply obtained if the $Ranf_I$ is much greater than zero.

c. Validation of the collision scheme. As a first problem chosen for validation the ISBT scheme, let us consider a square lid-driven cavity, shown in Fig. 4(a). Fig. 4(b) represents the accuracy of the ISBT collision scheme relative to its other counterparts, the SBT and NN schemes in prediction of the velocity components along the cavity center lines. However, in order to look deeper than the hydrodynamic properties allow, we need to investigate the collision frequency of the ISBT scheme in an equilibrium state in which the lid-driven velocity is set to zero, while the cavity wall surface and bulk gas have the same temperature equal to 273 K. In this state, the equilibrium collision rate per molecule is given theoretically (CF_{th}) by[2]

$$CF_{th} = 4nd_{ref}^2\sqrt{\frac{\pi K_B T_{ref}}{m_s}}\left(\frac{T}{T_{ref}}\right)^{1-\omega}, \tag{9}$$

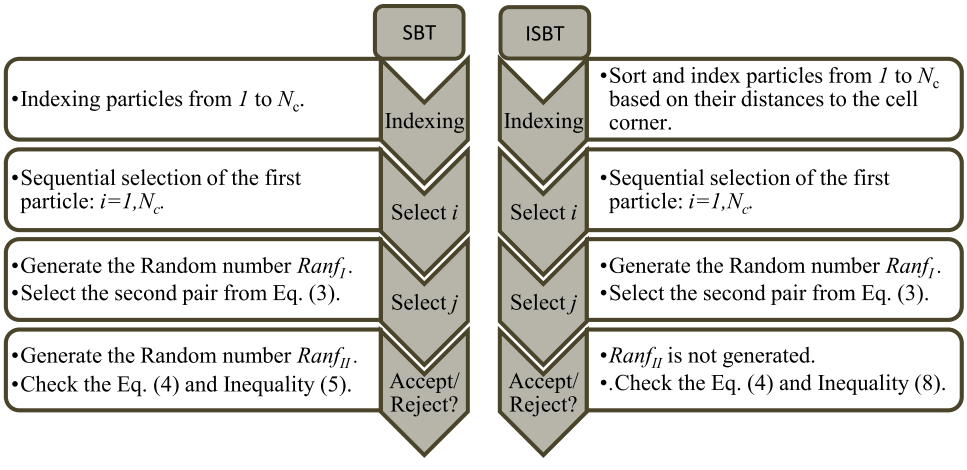

FIG. 2. The simplified Bernoulli trials (SBT) and the intelligent simplified Bernoulli trials (ISBT) collision schemes, compared by their collision procedures.

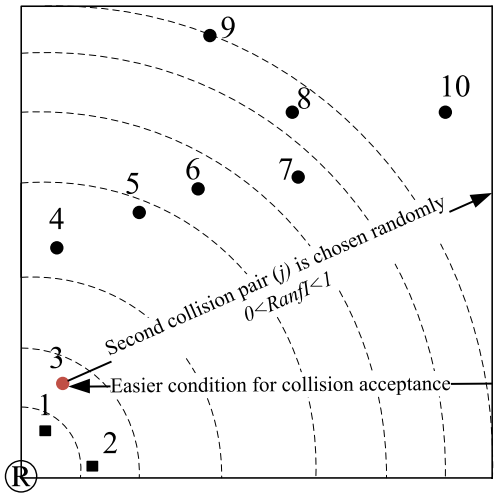

FIG. 3. Pseudo-circular subcells in the ISBT scheme that causes a biased selection for closer collision pairs.

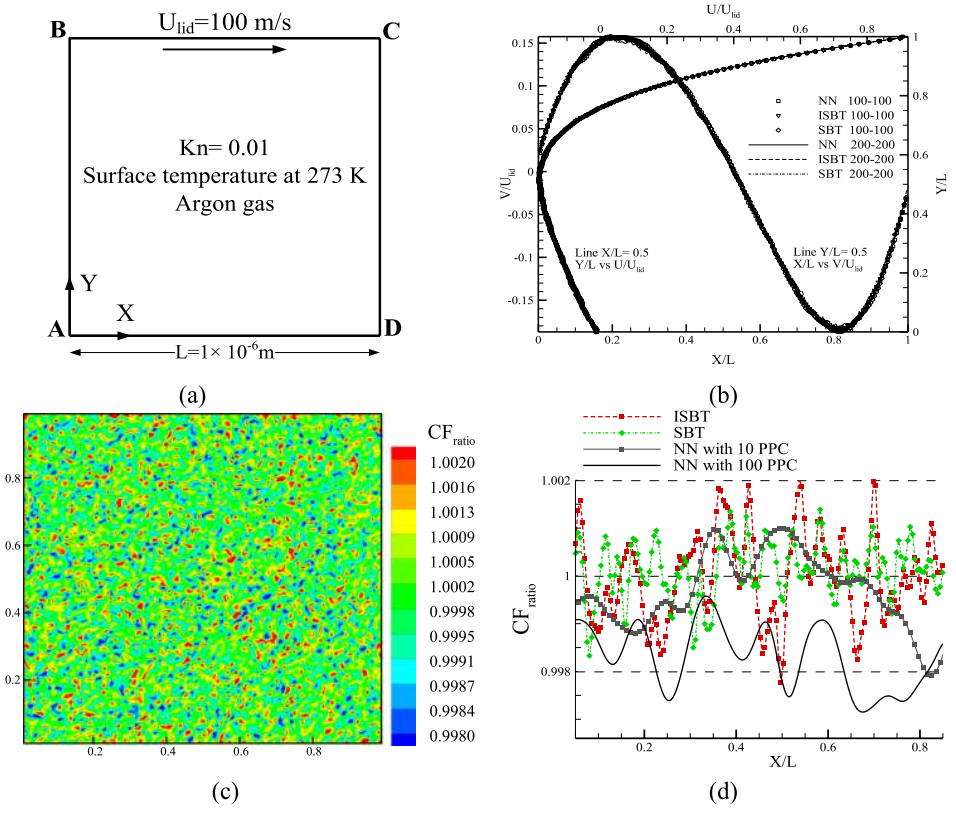

FIG. 4. (a) The lid-driven cavity used to investigate the validation of the ISBT scheme, (b) comparison of velocity components of the lid-driven cavity along the center lines, between NN, ISBT, and SBT schemes, in two different division grids of 100×100 and 200×200 with 10 particles per collision cell, (c) contour of CF_{ratio} in the cavity at the equilibrium state, using the 100×100 grid and 10 particles per cell, calculated by the ISBT scheme, and (d) CF_{ratio} along the horizontal center line calculated by the NN, ISBT, and SBT schemes.

TABLE I. Comparison of the $SOF(\frac{MCS}{\lambda})$ value in the lid-driven cavity flow between NN, ISBT, and SBT collision schemes.

Collision scheme	Division size	*SOF* value	*SOF* normalized by the resembling NN value	*SOF* normalized by the resembling SBT value
NN	100-100	0.0477	1	0.182
ISBT	100-100	0.1740	3.66	0.666
SBT	100-100	0.2621	5.49	1

where n, d_{ref}, K_B, T_{ref}, m_s, and ω are number density, gas molecular reference diameter, Boltzmann constant, reference temperature, molecular mass, and viscosity-temperature exponent, respectively. CF_{num} represents the numerical value of this rate that is calculated by the division of the number of collisions in each cell (N_{coll}) on the execution time (*Time*) and half of the mean particle numbers per cell (0.5 N_p) as follows:

$$CF_{num} = \frac{N_{coll}}{0.5 N_p Time}. \tag{10}$$

CF_{ratio} is the ratio of the CF_{num} to its theoretical value in equilibrium state. Here, this ratio must have a magnitude close to unity. Fig. 4(c) demonstrates the ability of the ISBT scheme to correctly predict the number of collisions, and Fig. 4(d) states that the deviation of the CF_{ratio} from the unity in the ISBT collision scheme, similar to other schemes, is bounded with acceptable limit of 0.002. When the number of particles per cell increases, the NN solution shows a very slight underestimation of the number of collisions. The dimensionless number, *SOF* (separation on freepath), which is the mean collisional separation (*MCS*) distance divided by the local mean free path (λ), i.e., $SOF = MCS/\lambda$, is selected as a parameter for measuring the quality of collisions. Table I shows that the ISBT, compared with the SBT collision scheme, reduces the *SOF* value about one-third.

III. RESULTS AND DISCUSSION

In this section, the investigations performed on different test cases such as Mach 10 lid-driven cavity flow, steady hypersonic flow over a cylinder, and hypersonic flow over the 25°–55° biconic are presented. The nitrogen and argon molecular gas constants used in the current studies are those given in Ref. 2. The values of the viscosity temperature power index (ω) of argon and nitrogen gases are 0.81 and 0.74, respectively. In case of nitrogen, a rotational relaxation collision number of 5 and a temperature-dependent vibrational collision number (Eq. (6.53) of Ref. 2) are used.

A. Mach 10 lid-driven cavity flow

The indexing method of the ISBT collision scheme (presented in the Fig. 1(a)) might cause some discrepancies between the ideal random selection of particles (e.g., in the SBT or NN schemes) and closer-partner biased selections (e.g., in the ISBT scheme). Since, at each collision process, the ISBT particle indexing depends on distances to a definite point, there is a concern that in high-speed vortical flows, the ISBT collision scheme would not be able to correctly predict the hydrodynamic properties, specifically the angular momentum. Therefore, a forced vortex flow of the lid-driven cavity, filled with argon gas, at Kn = 0.01, T_w = 300 K, and U_{lid} = 3076.67 m/s is selected to ensure a condition of high-velocity flow with high vorticity. The simulations are conducted in the quadrangular collision cell-grids of 200×200 ($\lambda/2$) with 40 *PPC* (particles per collision cell) and 400×400 ($\lambda/4$) with 20 *PPC* as a benchmark case solved by the DS2V NN method. Fig. 5(a) denotes an acceptable accuracy of the ISBT scheme, in comparison with the NN method, in predicting the contour of temperature in the lid-driven cavity. Pressure and temperature distributions of the ISBT and the NN schemes along the horizontal and vertical centerlines of the

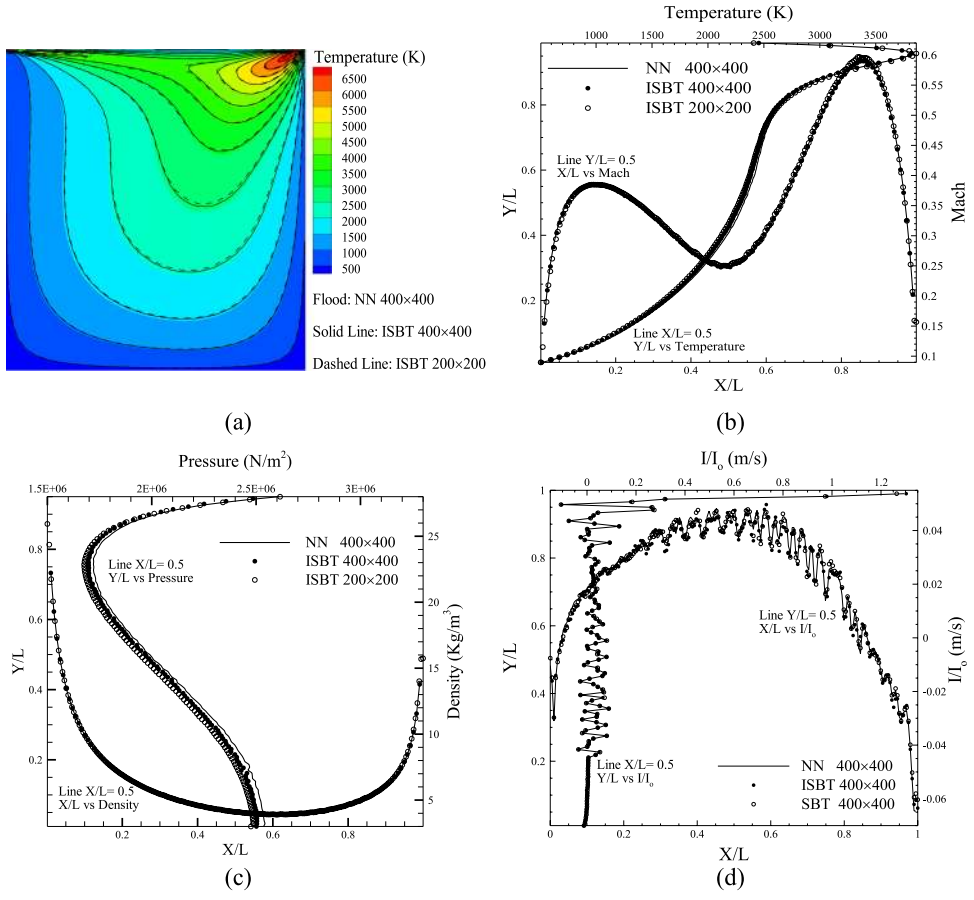

FIG. 5. The comparison of ISBT and NN, (a) contours of temperature (K), (b) the profile of temperature through the vertical centerline and the Mach line through the horizontal centerline, (c) the profile of pressure through the vertical centerline and the density line through the horizontal centerline, and (d) the profiles of angular momentum divided by I_o along the horizontal and vertical centerlines, in the domain of the lid-driven cavity flow (Mach 10, Kn = 0.01).

cavity are depicted in Figs. 5(b) and 5(c). Angular momentum (I) divided by a constant number of I_o, which is the product of the molecular mass and the cavity length ($m_s \bullet L$), is shown in Fig. 5(d). This profile implies that ISBT similar to other collision schemes (the NN and SBT) can predict the correct angular momentum. Furthermore, as it was stated in Section II A 2 b quadrangular cells are likely to index sequent-particles with the available maximum distance (located on the opposite corners of the "AC" diagonal in Fig. 1(d)). Here, in Fig. 5(d) we observed that this issue does not have a negative effect on the accuracy of the results; however, it might oblige the DSMC method to obtain larger sample-sizes to compensate the wrong collisions. This issue will be further investigated in Secs. III B and III C.

Alike the cavity problem in the validation Section II A 2 c here we also recognized a reduction of about 25%–32% of the MCS distance in the ISBT method compared with its similar cases in the SBT scheme.

B. Steady hypersonic flow over the cylinder

Hypersonic cylinder is a well-known 2D-benchmark.[19–21,23,24,28,31,32] It is a Mach 10 (2634.1 m/s) flow of argon at T = 200 K passing over a 12 in. circular cylinder with a fully diffusive surface at T_s = 500 K and a nominal free-stream Knudsen number of 0.01.

Fig. 6 illustrates the computational domain and the employed boundary conditions. Hypersonic flow past a cylinder is a test case with rapid variations in collision frequency and mean free path

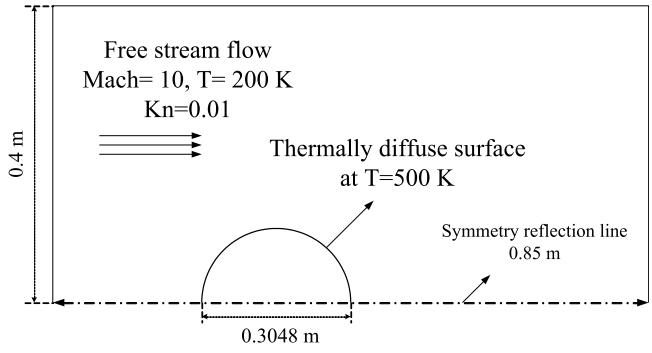

FIG. 6. Geometry of 2D hypersonic cylinder.

(λ), which requires the use of an adaptive grid.[31] The authors had already implemented the TAS technique, combined with the SBT scheme, with this test case (see Refs. 23 and 24). In this work, we implement ISBT-TAS scheme along with the achievements of Refs. 23 and 24, e.g., the surface properties filter weighted by surface sample sizes is used to reduce the microscopic fluctuations posed by the collision scheme. It has been observed that even when NN benefits from the aforementioned filter, this scheme needs collision and sample cell adaptation to reach the *exact* benchmark values. Therefore, specifically, in this test case, we focus our performance evaluations between the two SBT-TAS and ISBT-TAS schemes. The benchmark results are obtained by the NN collision scheme with the division grid of 194×100 and 20 initial *PPC*, and using the adaptation of collision and sample cell (run A1 in Table II). Table II presents the available runs, used in this study, in which B1-2 and C1-3 are obtained by the SBT-TAS and ISBT-TAS schemes, respectively. They provide good scales for accuracy and performance comparisons of the two SBT-TAS and ISBT-TAS schemes, for instance, one can see that the *SOF* is reduced about 31% between the two similar runs of B1 and C1.

Fig. 7 implies that all the available runs in this section have a high degree of accuracy on predicting surface properties. Fig. 8 compares the contour values of the three referenced runs (A1 without adaptation, B1, and C1) of the three schemes of NN, SBT-TAS, and ISBT-TAS.

In performance evaluation, first we found the minimum initial simulation resources of the two ISBT-TAS and SBT-TAS schemes (the division grid of 80×80 and 35 initial *PPC*). Then, we sought for the largest possible subcell sizes of the TAS system, for which the surface properties, illustrated in Fig. 7, remain highly accurate. The investigations showed that ISBT-TAS can operate with larger subcell sizes, so its TAS system adapts the collision cell to 6 particles ($PPSC = 6$), while in SBT-TAS, it does to 5 particles ($PPSC = 5$). Simulations continued until all their surface properties reach the accuracy presented in Fig. 7. During the simulation, all the sample-sizes, including the initiated ones, are considered. Table III provides the final output of this performance test; from the both perspectives of central processing unit (CPU)-time and DSMC sample-size, it is evident that runs C2-3 (belonged to ISBT-TAS) are more efficient than run B2 (belonged to SBT-TAS),

TABLE II. Simulation cases for the steady hypersonic cylinder.

Run name	Scheme	Division size	Initial *PPC*	Particles per sample cell adaption	Particles per collision cell adaption	*SOF* (MCS/λ)	*PPSC* adaptation in TAS	Subcell elongation factor *m*
A1	NN DS2V	194×100	20	24	8	0.063	1	1
B1	SBT-TAS	194×100	20	…	…	0.147	5	1
B2	SBT-TAS	80×80	35	…	…	0.191	5	1
C1	ISBT-TAS	194×100	20	…	…	0.101	5	2
C2	ISBT-TAS	80×80	35	…	…	0.156	6	2
C3	ISBT-TAS	80×80	35	…	…	0.159	6	1

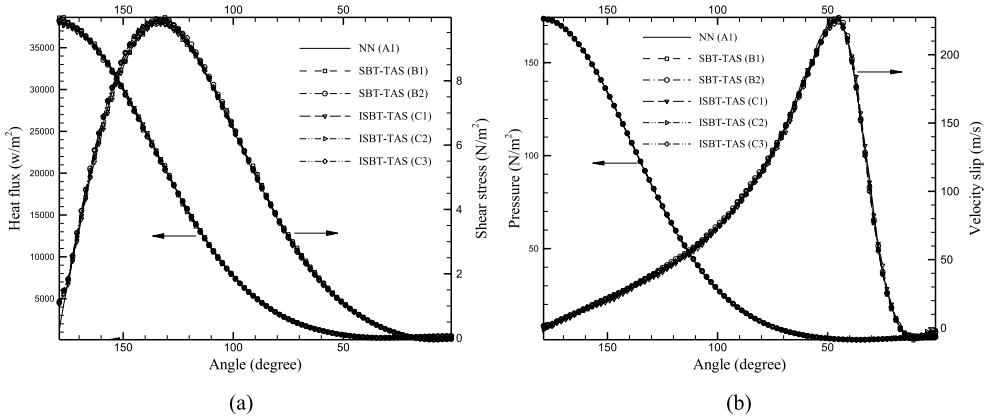

FIG. 7. ((a) and (b)): Comparison of surface properties in the cylinder flow problem for runs defined in Table II.

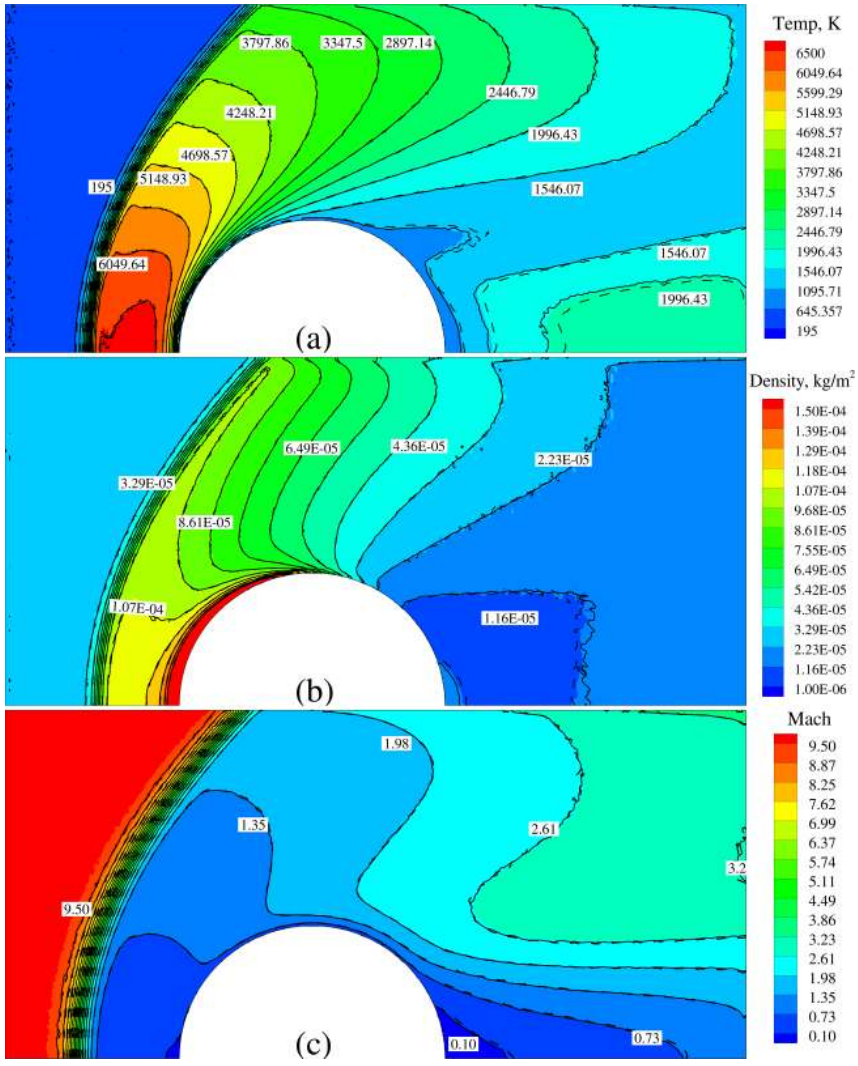

FIG. 8. Contours of (a) total temperature (K), (b) density (kg/m^3), and (c) Mach number, for runs defined in Table II, run A1 (flood) *without cell adaptation*, run B1 (dashed line), and run C1 (solid line).

TABLE III. Performance test results of runs B2 and C2-3. The system used for these tests has a 12 core CPU with the clock-speed of 3.4 GHz, and the RAM memory of 24 GB.

Run name	CPU-time (min)	Sample size	Normalized CPU-time	Normalized sample size
B2	309	1.9903×10^{10}	1	1
C2	248	0.8564×10^{10}	0.802	0.43
C3	210	0.9791×10^{10}	0.679	0.49

while this gap is bigger in sample sizes. Furthermore, the comparison of C2-3 connotes that the non-elongated subcell (C3) is more efficient than the elongated one (C2) from the viewpoint of CPU-time. Another point is that while the time step of C2 is reduced about one-third (see Section II A 2 b), its sample-size is also lower than C3.

1. ISBT time step values in a typical hypersonic cylinder test case

Here, we should note that except the runs with elongated subcells, all other simulations reported in Secs. III A and III B are obtained using the default values of DS2V, e.g., the same time step values were used for ISBT, SBT, and NN collision schemes. During these simulations, we observed that there is no need to reduce time step values for ISBT/SBT-TAS methods compared to NN; for instance, in case of the hypersonic flow over the cylinder with division size of 80×80 and an initial number of particles of 8.0×10^5, we compared simulations time step for NN, ISBT-TAS, and SBT-TAS, see Table IV.

C. Hypersonic flow over 25°–55° double-cone

The hypersonic nitrogen flow of Mach 15.6 passing over a 25°–55°degree biconic geometry contains quite demanding conditions consisting of a laminar recirculation zone, laminar expanding zone, high-speed low-density region, and low-speed high-density region. The North Atlantic Treaty Organization Research Technology Organization (RTO) under the coordination of Working Group 10 (Ref. 33) conducted some experimental studies on this test case. Additionally, Holden *et al.*[34] performed this experiment in the Calspan–University at Buffalo Research Center (CUBRC) 48-Inch Shock Tunnel. Here, we use the obtained experimental results from their tests. A DS2V investigation of this test case has been performed by Moss and Bird.[35] The accuracy and performance of the ISBT-TAS and SBT-TAS schemes will be compared with their validated counterpart in the DS2V code, the NN scheme. Biconic freestream conditions used in the CUBRC test facilities are given in Table V. Fig. 9(a) presents the biconic geometry and Fig. 9(b) illustrates a physical description of various shock wave types that occur over the geometry.[38]

In Sec. III B (the steady hypersonic cylinder), we mainly discussed the two ISBT-TAS and SBT-TAS schemes. Here, the objective is to study the performance and efficiency of the ISBT-TAS scheme against the SBT-TAS and specially the NN. In doing so, Table VI defines the conducted simulations which will further be used in our performance comparisons, and Figs. 10(a) and 10(b)

TABLE IV. Comparison of time step values between NN, SBT-TAS, and ISBT-TAS collision schemes in the steady hypersonic cylinder problem.

Collision method	Reported Time	Average time step	Time step at the reported time	Min. collision cell time step	Max. collision cell time step
NN	4.101×10^{-2}	6.684×10^{-7}	2.406×10^{-7}	6.684×10^{-8}	6.684×10^{-6}
ISBT-TAS	3.642×10^{-2}	6.237×10^{-7}	2.245×10^{-7}	6.237×10^{-8}	6.237×10^{-6}
SBT-TAS	3.910×10^{-2}	6.273×10^{-7}	2.258×10^{-7}	6.273×10^{-8}	6.273×10^{-6}

TABLE V. Freestream conditions for biconic problem.

Gas	V_∞ (m/s)	n_∞ (m^{-3})	$T_{\infty,T}$ (K)	ρ_∞ (kg/m^3)	P_∞ (N/m^2)	M_∞	Re_∞ (m^{-1})
N_2	2073	3.779×10^{21}	42.6	1.757×10^{-4}	2.23	15.6	$1.374\,67 \times 10^5$

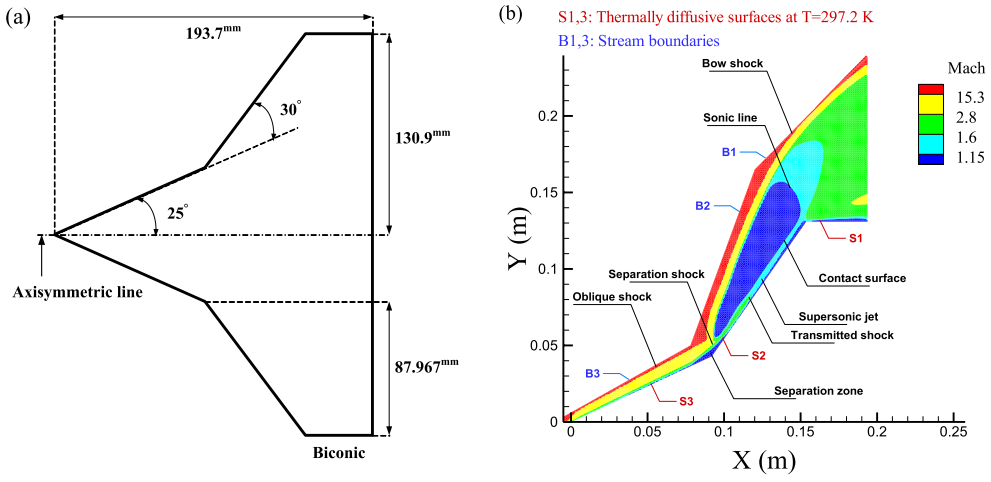

FIG. 9. (a) Biconic geometry and dimensions and (b) numerical domain and physical description.

TABLE VI. Simulation cases for the hypersonic biconic problem.

Run name	Scheme	Divisions size	Initial *PPC*	Total initial number of particles	*SOF* (MCS/λ)	*PPSC* adaptation in TAS	Subcell elongation factor *m*
A1	NN DS2V	160×195	54.9	1.3×10^6	0.232	1	1
B1	SBT-TAS	160×195	80.3	1.9×10^6	0.377	5	1
C1	ISBT-TAS	160×195	54.9	1.3×10^6	0.355	6	2
C2	ISBT-TAS	130×156	130.1	2.0×10^6	0.288	6	1

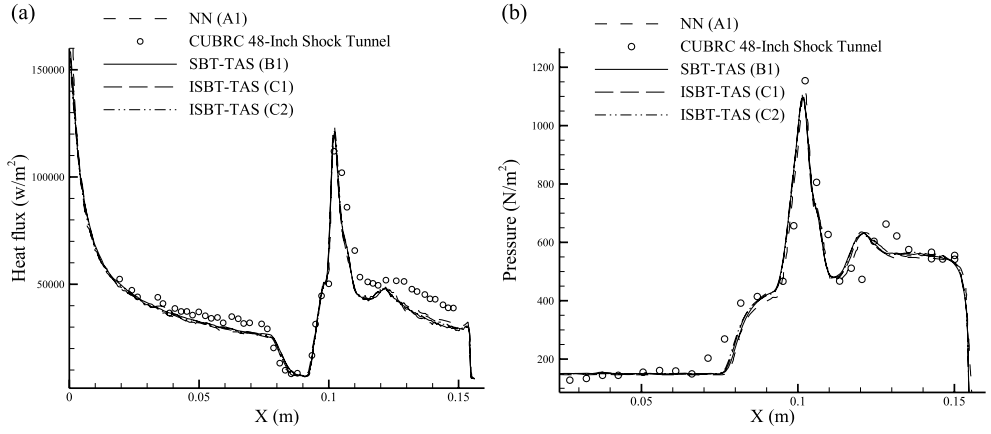

FIG. 10. ((a) and (b)): Comparison of surface properties in the biconic flow problem, including the simulations stated in Table VI and the CUBRC experimental data.

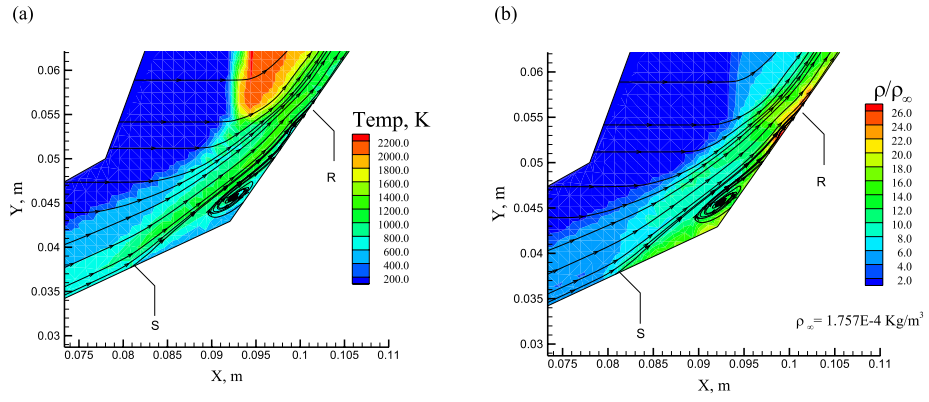

FIG. 11. ISBT-TAS contours of (a) temperature (K) and (b) normalized density in the separation region.

TABLE VII. Performance test results for runs stated in Table VI. The system used for these tests has a 12 core CPU with the clock-speed of 3.4 GHz and the RAM memory of 24 GB.

Run name	CPU-time	Sample size	Normalized CPU-time	Normalized sample size	$\Delta_{separation}$ (mm)	$\Delta_{reattachment}$ (mm)	Δ_R (mm)
A1	23 h:34 min	3.363×10^{10}	1	1	80.40	102.050	21.65
B1	30 h:28 min	1.938×10^{10}	1.292	0.582	80.23	101.844	21.61
C1	26 h:34 min	1.091×10^{10}	1.127	0.324	80.48	102.260	21.78
C2	34 h:20 min	1.566×10^{10}	1.456	0.465	80.35	101.973	21.62

depict their results over the biconic surface. The profiles presented in this figure states a suitable agreement of the calculations with the available CUBRC experimental data.

Similarly, the referenced runs in Table VI illustrated a suitable agreement on their inflow properties. Figs. 11(a) and 11(b) show ISBT-TAS different flow contours in the separation zone.

In order to evaluate the computational costs, the performance test passes this track: all the simulations defined in Table VI start and continue their calculations until they reach the stop point, when the converged length of the recirculation point (Δ_R) becomes greater than the resolved size of the recirculation zone (21.5 mm);[39] in other words,

$$\Delta_R = \left(X_{reattachment} - X_{separation}\right) > 21.5\ \text{mm},$$

during the simulation all the sample-sizes, including the initiated ones are considered.

Table VII presents the output of this performance test. Again, it is observed that ISBT-TAS works better if elongated subcells are employed (compare the C1-2 runs). Also the required sample size for the ISBT-TAS scheme is smaller than other methods. Considering the fact that the number of sample size is directly related to the number of iterations or collisions, it is possible to say that ISBT-TAS can register more accurate collisions and prevent from more unphysical ones. However, contrary to the NN method, which fundamentally obeys the NTC[2,36] to check for the maximum collision rate per time step, the ISBT/SBT collision procedure checks for all the available number of collisions. Therefore, from the viewpoint of CPU-time, which depends on the amount of numerical calculations, NN seems to be faster than other methods in this test case. Furthermore, in ISBT-TAS, it became possible to use less amount of resources than SBT-TAS scheme, e.g., run C1 used a smaller number of particles and run C2 used a coarser grid.

IV. CONCLUSIONS

The SBT collision scheme is designed to catch the correct collision frequencies with the minimum admissible number of particles. Besides the SBT's achievements toward this goal,[8–12] this scheme was modified to capture closer separated pair collisions. In this work, we introduced a

modified version of this scheme, the ISBT scheme, which has a semi-perception of inter-particle distances and can prioritize the acceptance of closer pairs. In the first step, to validate the method, we investigated the frequency and separation distances of collisions in a cavity at equilibrium state. We noticed that ISBT, compared to the SBT scheme, can reduce the MCS by approximately 25%–32%. We used a high velocity lid-driven cavity to reply to the concerns of the reduction of the angular momentum in the ISBT scheme. We then implemented the TAS technique to investigate the ISBT-TAS over some hypersonic flow test cases. All performed tests denote that, compared to the NN and SBT-TAS methods, the ISBT-TAS scheme requires the least possible sample-size amount preserving the same accuracy.

A future goal of our following investigations is to implement the ISBT-TAS scheme in three-dimensional space.

ACKNOWLEDGMENTS

The authors from Ferdowsi University of Mashhad would like to acknowledge the financial supports provided by the Faculty of Engineering, Ferdowsi University of Mashhad under Grant No. 30636.

[1] G. A. Bird, *Molecular Gas Dynamics* (Oxford University Press, Oxford, 1976).
[2] G. A. Bird, *Molecular Gas Dynamics and the Direct Simulation of Gas Flows* (Oxford University Press, Oxford, 1994).
[3] W. Wagner, "A convergence proof for Bird's direct simulation Monte Carlo method for the Boltzmann equation," J. Stat. Phys. **66**(3-4), 1011–1044 (1992).
[4] K. Koura, "Null - collision technique in the direct - simulation Monte Carlo method," Phys. Fluids (1958-1988) **29**(11), 3509–3511 (1986).
[5] M. Ivanov and S. Rogasinsky, "Theoretical analysis of traditional and modern schemes of the DSMC method," in *Proceedings of the 17th Symposium on Rarefied Gas Dynamics*, edited by A. Beylich (VCH, New York, 1990), pp. 629–642.
[6] O. M. Belotserkovskii and V. E. Yanitskii, "The statistical particles-in-cells method for solving rarefied gas dynamics problems," U.S.S.R. Comput. Math. Math. Phys. **15**, 101–114 (1975).
[7] V. E. Yanitskiy, "Operator approach to direct simulation Monte Carlo theory in rarefied gas dynamics," in *Proceedings of the 17th Symposium on Rarefied Gas Dynamics*, edited by A. Beylich (VCH, New York, 1990), pp. 770–777.
[8] S. K. Stefanov, in *Particle Monte Carlo Algorithms with Small Number of Particles in Grid Cells in Numerical Methods and Applications*, Lecture Notes in Computer Science edited by I. Dimov (Springer, 2011), Vol. 6046, pp. 110–117.
[9] S. K. Stefanov, "On DSMC calculation of rarefied gas flows with small number of particles in cells," J. Sci. Comput. **33**(2), 677–702 (2011).
[10] A. Amiri, E. Roohi, H. Niazmand, and S. Stefanov, "DSMC simulation of low Knudsen micro/nano flows using small number of particles per cells," J. Heat Transfer **135**(10), 01008 (2013).
[11] A. Shoja-Sani, E. Roohi, M. Kahrom, and S. Stefanov, "Investigation of rarefied gas flow around NACA 0012 airfoils using DSMC and NS solvers," Eur. J. Mech., B: Fluids **48**, 59–74 (2014).
[12] A. Saadati and E. Roohi, "Detailed investigation of flow and thermal field in micro/nano nozzle using simplified Bernouli trial (SBT) collision scheme in DSMC," Aerosp. Sci. Technol. **46**, 236–255 (2015).
[13] G. J. LeBeau, K. A. Boyles, and F. E. Lumpkin, "Virtual sub-cells for the direct simulation Monte Carlo method, American Institute of Aeronautics and Astronautics," AIAA Paper 2003-1031, 2003.
[14] G. A. Bird, "Direct simulation of high vorticity gas flows," Phys. Fluids **30**, 364–366 (1987).
[15] S. Stefanov, I. D. Boyd, and C.-P. Cai, "Monte Carlo analysis of macroscopic fluctuations in a rarefied hypersonic flow around a cylinder," Phys. Fluids **12**, 1226–1239 (2000).
[16] S. Stefanov, V. Roussinov, and C. Cercignani, "Rayleigh–Bénard flow of a rarefied gas and its attractors. I. Convection regime," Phys. Fluids **14**, 2255–2269 (2002).
[17] G. A. Bird, Visual DSMC Program for Two-Dimensional and Axially Symmetric Flows, The DS2V Program User's Guide, Version 2.1, G.A.B. Consulting Pty Ltd, Sydney, Australia, 2003.
[18] G. A. Bird, "The DS2V/3V program suite for DSMC calculations," AIP Conf. Proc. **762**, 541–546 (2005).
[19] C. C. Su, K. C. Tseng, H. M. Cave, J. S. Wu, Y. Y. Lian, T. C. Kuo, and M. C. Jermy, "Implementation of a transient adaptive sub-cell module for the parallel-DSMC code using unstructured grids," Comput. Fluids **39**, 1136–1145 (2010).
[20] C. C. Su, J. S. Wu, M. C. Lo, and F. A. Kuo, "Development of parallel direct simulation Monte Carlo method using a cut-cell Cartesian grid on a single graphics processor," Comput. Fluids **101**, 114–125 (2014).
[21] J. M. Burt, E. Josyula, and I. D. Boyd, "Novel cartesian implementation of the direct simulation Monte Carlo method," J. Thermophys. Heat Transfer **26**(2), 258–270 (2012).
[22] A. Amiri, E. Roohi, S. Stefanov, H. Nami, and H. Niazmand, "DSMC simulation of micro/nano flows using SBT-TAS technique," Comput. Fluids **102**, 266–276 (2014).
[23] B. Goshayeshi, E. Roohi, S. Stefanov, and J. A. Esfahani, "Extension of the SBT-TAS algorithm to curved boundary geometries," AIP Conf. Proc. **1628**, 266–275 (2014).
[24] B. Goshayeshi, E. Roohi, and S. Stefanov, "DSMC simulation of hypersonic flows using an improved SBT-TAS technique," J. Comput. Phys. **303**, 28 (2015).

[25] M. A. Gallis, J. R. Torczynski, D. J. Rader, and G. A. Bird, "Convergence behavior of a new DSMC algorithm," J. Comput. Phys. **228**(12), 4532–4548 (2009).
[26] M. A. Gallis and J. R. Torczynski, "Effect of collision-partner selection schemes on the accuracy and efficiency of the direct simulation Monte Carlo method," Int. J. Numer. Methods Fluids **67**(8), 1057–1072 (2011).
[27] M. A. Gallis, J. R. Torczynski, D. A. Levin, I. J. Wysong, and A. L. Garcia, "Efficient DSMC collision-partner selection schemes," AIP Conf. Proc. **1333**(1), 248 (2011).
[28] G. A. Bird, *The DSMC Method* (CreateSpace Independent Publishing, Platform, USA, 2013).
[29] G. A. Bird, M. A. Gallis, J. R. Torczynski, and D. J. Rader, "Accuracy and efficiency of the sophisticated direct simulation Monte Carlo algorithm for simulating noncontinuum gas flows," Phys. Fluids **21**(1), 017103 (2009).
[30] M. A. Gallis, J. R. Torczynski, D. J. Rader, and G. A. Bird, "An improved - accuracy DSMC algorithm," AIP Conf. Proc. **1084**(1), 299–304 (2008).
[31] A. J. Lofthouse, I. D. Boyd, and J. M. Wright, "Effects of continuum breakdown on hypersonic aerothermodynamics," Phys. Fluids **19**, 027105 (2007).
[32] C. C. Su, K. C. Tseng, J. S. Wu, H. M. Cave, M. C. Jermy, and Y. Y. Lian, "Two-level virtual mesh refinement algorithm in a parallelized DSMC code using unstructured grids," Comput. Fluids **48**, 113–124 (2011).
[33] D. Knight, "RTO WG 10: Test cases for CFD validation of hypersonic flight," AIAA Paper 2002-0433, 2003.
[34] M. S. Holden, T. P. Wadhams, G. V. Candler, and J. K. Harvey, "Measurements of regions of low density Laminar shock wave/boundary layer interactions in hypersonic flows and comparison with Navier–Stokes predictions," AIAA Paper 2003-1131, 2003.
[35] J. N. Moss and G. A. Bird, "Direct simulation Monte Carlo simulations of hypersonic flows with shock interactions," AIAA J. **43**(12), 2565–2573 (2005).
[36] G. A. Bird, "Comment on 'False collisions in the direct simulation Monte Carlo method' [Phys. Fluids 3 1, 2047 (1988)]," Phys. Fluids A **1**(5), 897–897 (1989).
[37] S. Stefanov and C. Cercignani, "Monte Carlo simulation of Bénard's instability in a rarefied gas," Eur. J. Mech., B: Fluids **11**(5), 543–554 (1992).
[38] E. Titov, J. Burt, E. Josyula, and I. Nompelis, "Implications of slip boundary conditions on surface properties in hypersonic flows," AIAA Paper 2012-3307, 2012.
[39] J. K. Harvey, "A review of a validation exercise on the use of the DSMC method to compute viscous/inviscid interactions in hypersonic flow," AIAA Paper 2003-3643, 2003.